

1/f fluctuations of amino acids regulate water transportation in aquaporin 1Eiji Yamamoto,¹ Takuma Akimoto,¹ Yoshinori Hirano,^{2,3} Masato Yasui,² and Kenji Yasuoka¹¹*Department of Mechanical Engineering, Keio University, Yokohama, Japan*²*Department of Pharmacology, School of Medicine, Keio University, Shinjuku-ku, Tokyo, Japan*³*Laboratory for Computational Molecular Design, Computational Biology Research Core, Quantitative Biology Center (QBiC), The Institute of Physical and Chemical Research (RIKEN), Kobe, Japan*

(Received 27 August 2013; published 21 February 2014)

Aquaporins (AQPs), which transport water molecules across cell membranes, are involved in many physiological processes. Recently, it is reported that the water-water interactions within the channel are broken at the aromatic/arginine selectivity filter (ar/R region), which prevents proton transportation [U. K. Eriksson *et al.*, *Science* **340**, 1346 (2013)]. However, the effects of the conformational fluctuations of amino acids on water transportation remain unclear. Using all-atom molecular dynamics simulations, we analyze water transportation and fluctuations of amino acids within AQP1. The amino acids exhibit 1/f fluctuations, indicating possession of long-term memory. Moreover, we find that water molecules crossing the ar/R region obey a non-Poisson process. To investigate the effect of 1/f fluctuations on water transportation, we perform restrained molecular dynamics simulations of AQP1 and simple Langevin stochastic simulations. As a result, we confirm that 1/f fluctuations of amino acids contribute to water transportation in AQP1. These findings appreciably enhance our understanding of AQPs and suggest possibilities for developing biomimetic nanopores.

DOI: 10.1103/PhysRevE.89.022718

PACS number(s): 87.15.hj, 87.10.Tf, 87.14.ep, 87.15.Ya

I. INTRODUCTION

As current trends in population growth, industry, agriculture, and environmental issues place increasing demands on fresh water supplies, effective and selective water pores for desalination of salty water are becoming actively sought. Aquaporins (AQPs), transmembrane proteins found in the cell membranes of all living entities, are natural transporters of water molecules. Thirteen isoforms of human AQPs (AQP0-12) have been identified, each with a different tissue distribution, and each playing specific physiological roles [1,2]. All AQPs form tetramers in cell membranes, and some form large arrays with varying structural properties [3,4]. Most AQPs exclusively permit water molecules, rejecting charged molecules, ions, and even protons [5,6], while some AQPs can be permeated by molecules other than water [7,8]. Recently, a high resolution x-ray structure of yeast AQP (0.88 Å) reveals a feasible part to prevent proton permeation [9]. By understanding the mechanism of water transportation within AQPs, researchers can begin to design biomimetic nanopores for desalination processes [10–12].

The first structurally characterized AQP, AQP1, strictly transports water molecules [13]. Further insights into water configuration and the energetics of water permeation within AQPs has been provided by molecular dynamics (MD) simulations [5,14–18]. During transit through the AQP pore, water molecules rotate as they encounter regions that heavily polarize their dipoles. In carbon nanotubes (CNTs), water molecules diffuse single file by a continuous-time random walk process with exponential waiting time distribution [19]. On the other hand, the statistical properties of first-passage water transport times in OmpF membrane protein channels are known to differ from those in homogeneous pores such as CNTs [20]. Therefore, little is known about AQP water dynamics because the channel steric conformations of AQPs are much more complicated than those in CNTs.

As water molecules transit through AQPs, they are affected by neighboring water molecules and by AQP amino acids. Water–amino acid interactions occur chiefly in two characteristic domains, the NPA motif and the aromatic/arginine selectivity filter (ar/R region) [14]. Recently, Eriksson *et al.* reported that the water-water interactions within the yeast AQP are broken at the ar/R region, which prevents proton transportation [9]. Therefore, the ar/R region plays an important role in water transportation. However, the roles of fluctuations of the amino acids in these interactions are unclear. The relationship between conformational fluctuations of amino acids and water dynamics within AQPs may be of high biological importance.

In this paper, we perform MD simulations of the AQP1 embedded in a palmitoyl-oleoyl-phosphatidylethanolamine (POPE) bilayer [see Fig. 1(a)]. The amino acids in AQP1 are found to undergo 1/f fluctuations. Moreover, the occurrence of water molecules crossing the ar/R region of AQP1 is a non-Poisson process. Analyzing water transportation through the channel as modeled by Langevin stochastic simulations, we suggest that the 1/f fluctuations of amino acids may be implicated in water transportation control in AQPs.

II. METHODS**A. Molecular dynamics simulation**

To elucidate the water transport properties and fluctuations of amino acids in AQP1, we performed MD simulations of AQP1 (based on the x-ray crystallographic structure [21]) embedded in a POPE bilayer. The initial membrane system contained a homotetrameric assembly of free AQP1, 526 POPE molecules, and 74 738 TIP3P water molecules [see Fig. 1(a)]. Before MD simulation, we minimized the energy of the system by the steepest descent method followed by the conjugate gradient method. A 120 ns MD simulation of the

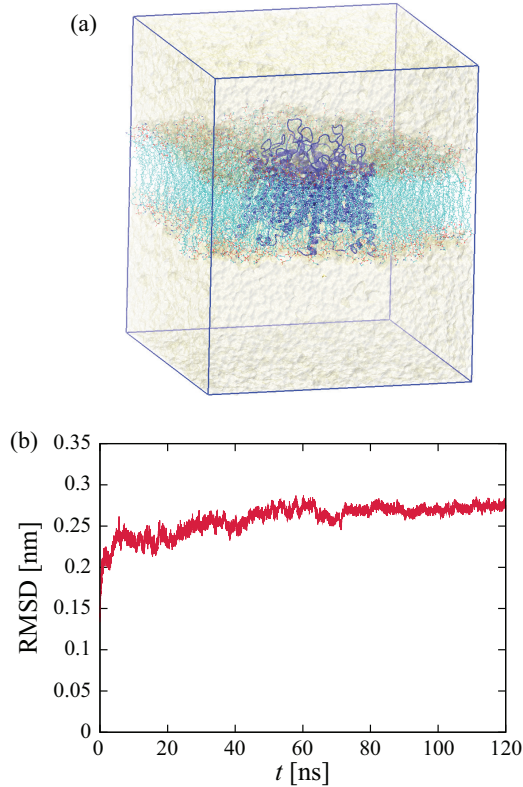


FIG. 1. (Color online) (a) The system used for MD simulations of AQP1 in a POPE lipid bilayer. A single tetramer of AQP1 is embedded in the POPE lipid bilayer. The AQP1 is shown in cartoon (blue). Lipids are shown in green with their oxygen atoms in red. Explicit water molecules correspond to the upper and lower transparent coatings. The blue line of the box is a periodic boundary. (b) Root-mean-square deviation (RMSD) of the AQP1. The RMSD fluctuates around a constant value after 70 ns, which means that the structure of the AQP1 is in an equilibrium.

system was performed with a constant number of atoms at a pressure of 0.1 MPa and a temperature of 310 K. The MD simulation was carried out using Berendsen's algorithm with a coupling time of 0.2 ps. The time step was set at 1 fs. The lengths of hydrogen bonds were constrained to equilibrium lengths using the SHAKE method. Parm99 and gaff parameters were used for the protein and POPE lipids, respectively. This parameter for POPE has been used in previous studies of membranes or membrane proteins [22–26]. The particle mesh Ewald method was used, with a specified direct space cutoff distance of 1.0 nm. A three-dimensional periodic boundary condition was imposed on all systems. Because the system reached equilibrium at 70 ns, the trajectories of the final 50 ns were used in the analysis [see Fig. 1(b)].

Moreover, to investigate the effect of the $1/f$ fluctuations of amino acids on water transportation, we performed three MD simulations in which all amino acid residues of AQP1 were restrained within a harmonic potential in Cartesian space. The force constant was 10 kcal/mol \AA^2 . The initial structures in the restrained MD simulations were assumed from equilibrium structures of MD simulations at 80, 100, and 120 ns. Three independent restrained MD simulations were performed over

20 ns. All MD simulations were performed using AMBER10 software [27].

B. Detrended fluctuation analysis

Detrended fluctuation analysis (DFA) [28] is a method for detecting a long-range correlation embedded in a time series. First, we construct an integrated time series $y_i = \sum_{j=1}^i r_j$ and divide the series into bins of size n . The fluctuation function $F(n)$ is the root mean square of the deviations from a local trend (determined by least-squares fitting), defined by

$$F(n) \equiv \sqrt{\frac{1}{mn} \sum_{j=1}^m \sum_{i=(j-1)n+1}^{jn} \{y_i - (a_j x_i + b_j)\}^2}, \quad (1)$$

where m represents the number of bins of size n . The fluctuation function exhibits a scaling $F(n) \simeq n^\beta$, and the scaling exponent β gives information about the correlation properties of the time series. The cases $\beta < 0.5$ and $\beta > 0.5$ correspond to anticorrelated and correlated noise, respectively. In particular, certain exponents β correspond to characteristic noises: $\beta \simeq 0.5$, white noise; and $\beta \simeq 1$, $1/f$ noise. The exponent β and the exponent α of the power spectral density $S(f) \simeq f^{-\alpha}$ of the original time series are related by $\alpha = 2\beta - 1$.

III. RESULTS AND DISCUSSION

A. Fluctuations of amino acids in AQP1

Channel steric conformation and solute binding sites in AQP1 facilitate the rapid and highly selective transportation of water molecules. As mentioned above, AQP1 contains two characteristic domains. One is the Asn-Pro-Ala (NPA) motif located at the two short helices in the center of the membrane, which contains amino acids N78 and N194 [21] [see Fig. 2(a)]. The NPA motif allows water molecules to form hydrogen bonds with two Asn residues, thereby reversing the orientation of the water molecules. The other domain is an ar/R region constituting the narrowest part of the pore, formed by Phe58, His182, Cys191, and Arg197 [17,29] [see Fig. 2(b)]. The ar/R region performs a filtering role, blocking partially hydrated ions that are too large to pass through the narrow region [6,22]. To evaluate the conformational fluctuations in AQP1, we analyze the distances between the centers of mass coordinates of amino acids in the ar/R region (H182 and R197) and in the NPA motif (N78 and N194) over a 50 ns simulation period [see Fig. 2(c)]. The distance fluctuations are characterized by the power spectral density of these distances [see Fig. 2(d)]. The amino acids in AQP1 show $1/f$ fluctuations. To improve the clarity of the results, we perform DFA [see Fig. 2(e)]. The $F(n)$ is linear about both H182-R197 and N78-N194, again suggesting that the distances between the amino acids undergo $1/f$ fluctuations. Power spectral density and DFA of shuffled time series of the distances between the amino acids signify a white noise (see Fig. 3). This implies that a long-term memory contributes to the $1/f$ fluctuation. Figure 2(f) shows a probability density function (PDF) of the power law exponent α . The distances between amino acid pairs show $1/f^\alpha$ fluctuations in AQP1. The exponent α depends on the amino acid pairs.

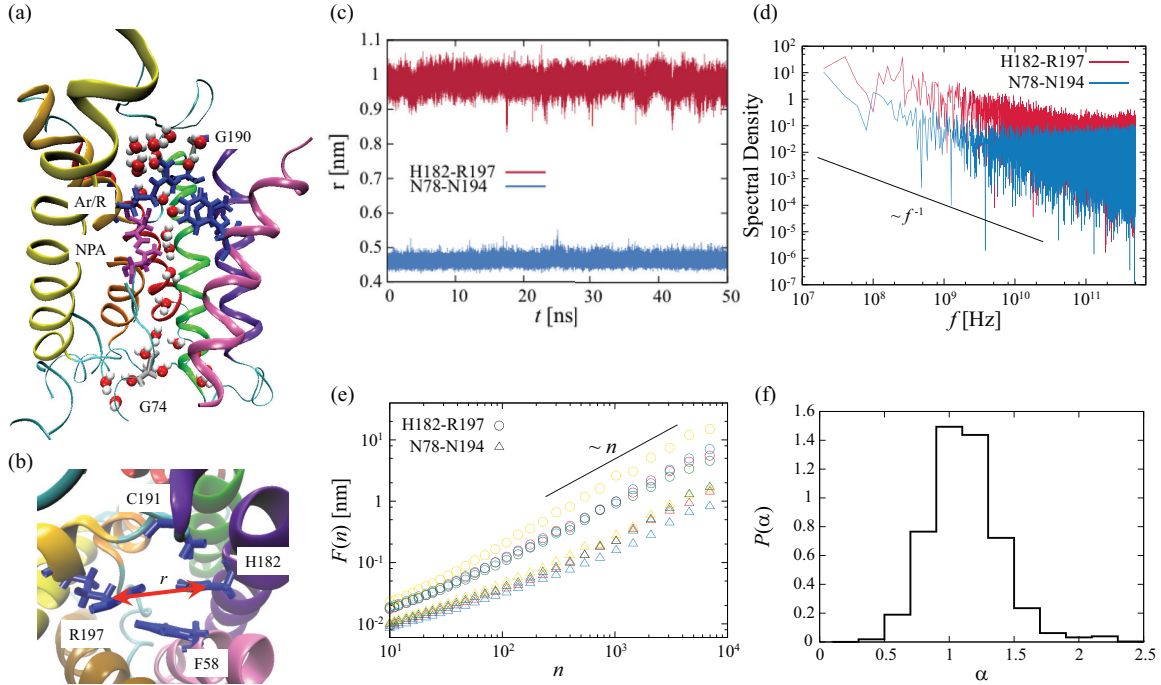


FIG. 2. (Color online) Fluctuations of amino acids in AQP1. (a) Snapshot of AQP1 monomer channeling a single file of water molecules. (b) Snapshot of ar/R region in AQP1. Histidine and arginine contribute to the filter mechanism. The distance between H182 and R197 is analyzed. (c) Distances between amino acids in AQP1, as a function of time. Red and blue lines indicate H182-R197 and N78-N194 distances, respectively. (d) Power spectral density of the distances between amino acids. The solid line has slope -1 . (e) DFA of distances between amino acids in AQP1. Different pores in the AQP1 tetramer are distinguished by colored symbols. Circles and triangles represent the H182-R197 and N78-N194 distances, respectively. The black line is shown for reference. (f) PDF of the exponent α of power spectral densities $S(f) \simeq f^{-\alpha}$ on amino acid distances. These are obtained from all amino acid pairs in a monomer.

These $1/f$ fluctuations of amino acids are intriguing. In biological systems, $1/f^\alpha$ noises have been reported for protein conformational dynamics [30,31], DNA sequences [32], and ionic currents [33–35], implying that biological proteins generally undergo long-range correlated dynamics. Distance fluctuations between donors and acceptors have been modeled by the generalized Langevin equation with fractional Gaussian noise [31]. Thus, we expect that other transmembrane proteins will exhibit $1/f$ fluctuations. Our present finding has potentially important implications for biological functions.

B. Water dynamics within AQP1

To investigate the water dynamics in AQP1, we calculate the free energy difference $F_e(z)$ of water molecules in the AQP1 pore, given by $F_e(z) = -\ln \rho(z)$ [see Fig. 4(a)], where z and $\rho(z)$ are the coordinate and the PDF, respectively, of water molecules in the pore. We define units of energy by setting $k_B T = 1$. The PDFs are computed from all trajectories of water molecules in four different pores. There is a high energy barrier around the ar/R region ($z \cong 0.6\text{--}0.8$ nm). Water molecules are trapped in a free energy valley in AQP1. Trapped water molecules jump to neighboring sites at certain instances in time. Jumping events are evident in the trajectories of water molecules in the AQP1 [see Fig. 4(b)]. To investigate the jumping event across the ar/R region, we define the z coordinate of this region as the center of mass of the H192 and R197 amino acids [the pink line in Fig. 4(b)]. Because the

ar/R region is the narrowest section of the pore, jumping events across the region are readily observed. We then calculate the PDFs of the interoccurrence times of the jumping events. To remove molecular vibrational effects from the PDF, an event is considered a jump only if its movement across the z coordinate of the ar/R region exceeds 0.1 nm. As shown in Fig. 4(c), the PDFs follow nonexponential distributions, a non-Poisson process.

One important question remains unclear: What is the origin of the non-Poisson process? In other words, does the non-Poisson process come from effects by the complex configuration within the pore or $1/f$ fluctuation of amino acids? To address this question, we perform MD simulations in which the AQP1 structure is restrained using a harmonic potential. Three independent restrained MD simulations are performed over 20 ns. DFAs of the NPA motif (N78 and N194) and ar/R region (H182 and R197) are shown in Fig. 5(a). The amino acid fluctuations are modified in the restrained MD simulations. Here, the line of slope 0.5 signifies white noise. Figure 5(b) shows $F_e(z)$ of water molecules in the restrained AQP1. The value of $F_e(z)$ depends on the first configuration used for the restrained MD simulations. The modified fluctuations from $1/f$ noise to white noise alter the water transportation dynamics within the AQP1. The jump events across the ar/R region are characterized by a Poisson process, where the interoccurrence times of the jumping events are distributed exponentially [see Fig. 5(c)]. This implies that water transportation is extensively affected by amino acid

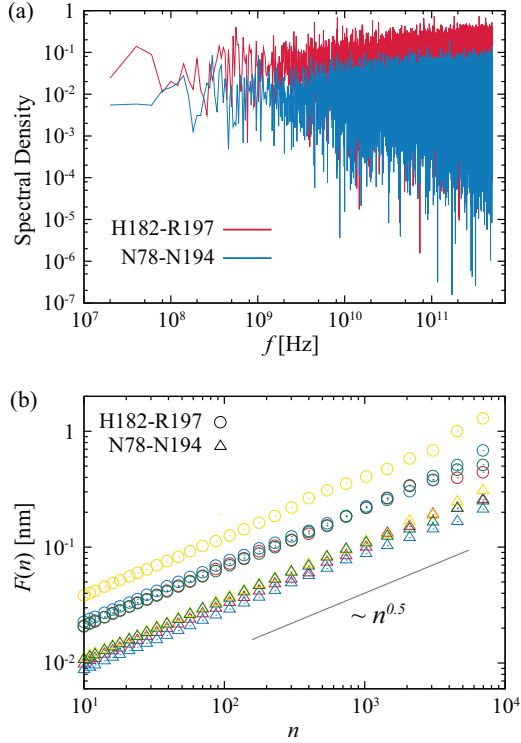


FIG. 3. (Color online) (a) Power spectra of shuffled time series of the distances between amino residues. We construct a time series by shuffling the original time series of the distance between amino residues in a random manner. Red and blue lines indicate H182-R197 and N78-N194 distances, respectively. (b) DFAs on shuffled time series of distances of amino residues in AQP1. Colored symbols distinguish the difference of AQP1 pores. Circles and triangles represent the distances of H182-R197 and N78-N194, respectively. The solid line represents $F(n) \sim n^{0.5}$, signifying white noise.

fluctuations. Because the water transportation depends largely on the pore size, the $1/f$ fluctuation of distances between amino acids within the AQP1 is important to regulate the water transportation. We note that the pore sizes in some restrained AQPs became too small to pass water molecules.

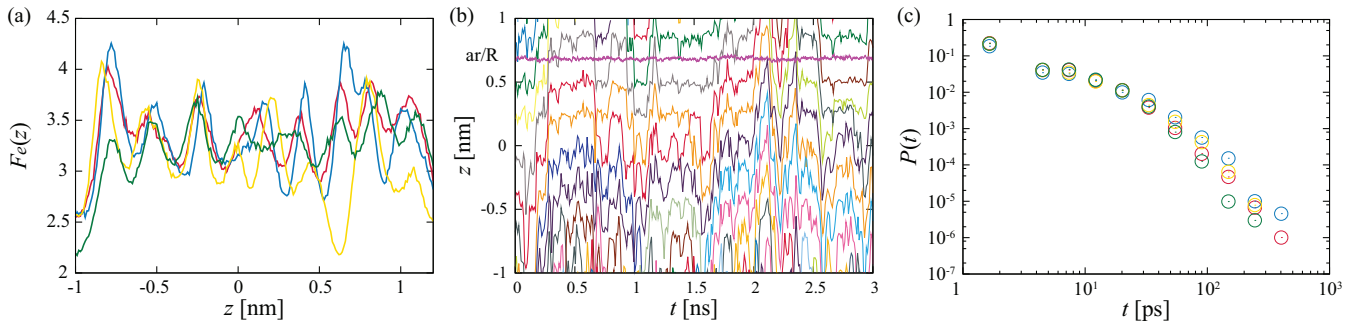


FIG. 4. (Color online) Water transportation in AQP1. (a) Free energy variation of water molecules within AQP1. The NPA motif (center of N78 and N194) is located at $z = 0$. Colored lines represent the density of water molecules in different pores of the AQP1 tetramer. (b) Water translocation in AQP1 throughout the 3 ns time course of the MD simulation. The z coordinate of the NPA motif (located at $z = 0$) has been subtracted from all z coordinates. For enhanced clarity, results are averaged over 10 ps intervals. Individual water molecules are assigned different colors each time they enter or reenter the channel. Pink line around $z = 0.7$ nm is the z coordinate of the ar/R region (center of H182 and R197). (c) PDFs of interoccurrence times of jump events of water molecules at the ar/R region. Different AQP1 pores are distinguished by colored symbols.

C. Stochastic model of water transportation

The restrained MD simulations are somewhat artificial and it is difficult to obtain enough ensembles due to the dependence on the first configuration. To capture the essential feature of water transportation through AQPs, we propose a stochastic model that a particle is trapped in a potential and jumps the potential height [see Fig. 6(a)]. As discussed in the previous section, events of water molecules crossing the ar/R region crucially depend on the pore size, which fluctuates with the $1/f$ distribution. The pore size corresponds to the height of the potential E , and the fluctuation of the amino acids represents the fluctuation of the potential height. We consider that the motion of water molecules is driven by white Gaussian noise. The water molecules are modeled as particles governed by a Langevin equation in a harmonic potential:

$$m \frac{d^2x(t)}{dt^2} = -m\gamma \frac{dx(t)}{dt} - kx(t) + R(t), \quad (2)$$

where m is the mass of water molecule, γ is a friction coefficient, and k is a spring constant. The random driving force $R(t)$ satisfies the fluctuation-dissipation relation $\langle R(t)R(t') \rangle = 2m\gamma k_B T \delta(t - t')$, where k_B is the Boltzmann constant and T is a temperature. Parameter values used in simulations were $k = 5$ and $m = \gamma = 1$. Water permeation occurs when the particle exceeds a random fluctuating threshold. To mimic $1/f$ fluctuations, a fluctuating threshold $E(t)$,

$$E(t) = E_0 + E_N(t), \quad (3)$$

is generated by the following method [36], where E_0 specifies an average threshold:

$$E_N(t) = \sum_{i=0}^{N-1} \zeta_i(t), \quad (4)$$

$$\frac{d\zeta_i(t)}{dt} = -\nu_i \zeta_i(t) + \sqrt{2\nu_i \eta_i c_N} \xi_i(t), \quad (5)$$

where $\nu_i = \nu_0/b^i$ is the inverse autocorrelation time of the i th component and $\eta_i = [\eta_\alpha / \Gamma(1 - \alpha)] C_\alpha(b) \nu_0^\alpha / b^{i\alpha}$ is its weight. The autocorrelation function of the noise is the sum of independent autocorrelation functions,

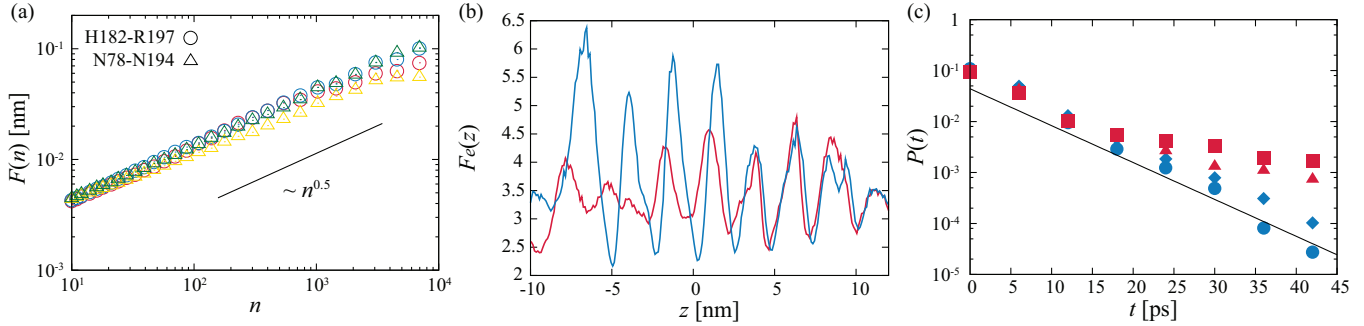


FIG. 5. (Color online) Restrained MD simulations of AQP1. (a) DFAs on distances of amino acids in AQP1. Colored symbols distinguish between different AQP1 pores. Circles and triangles represent H182-R197 and N78-N194 distances, respectively. The solid line represents $F(n) \sim n^{0.5}$. (b) Free energy variation of water molecules within restrained AQP1. The NPA motif is located at $z = 0$. Colored lines represent the density of water molecules in different pores. (c) PDFs of interoccurrence times of the jumping events of water molecules across the ar/R region. Red and blue (dark and light gray) symbols indicate the results of MD and restrained MD simulations, respectively. Different pores in the AQP1 tetramer are distinguished by different symbols. The solid line represents an exponential distribution.

$$\langle \zeta_i(t) \zeta_j(0) \rangle = c_N \eta_i \delta_{ij} \exp(-\nu_i t),$$

$$\langle E_N(t) E_N(0) \rangle = \sum_{i=0}^{N-1} c_N \eta_i \exp(-\nu_i t),$$

which approximates $1/f^{1-\alpha}$ noise. Parameter values used in simulations were $E_0 = 1.35$, $\nu_0 = 50$, $b = 10$, $\eta_\alpha = 0.5$,

$\alpha = 0.0001$, and $N = 16$. Power spectra of the $E_N(t)$ is shown in Fig. 6(b). In the case of $N = 1$, the PDF of escape times follows an exponential distribution for different ν_1 [Fig. 6(c)]. We note that the variance of $E_1(t)$ is adjusted to that of $N = 16$ by changing $\eta_1 c_1$. Figure 6(d) shows the PDF of escape times when the potential barrier fluctuates with $1/f$ noise ($N = 16$). In this case, the PDF follows a nonexponential distribution that strongly agrees with that of

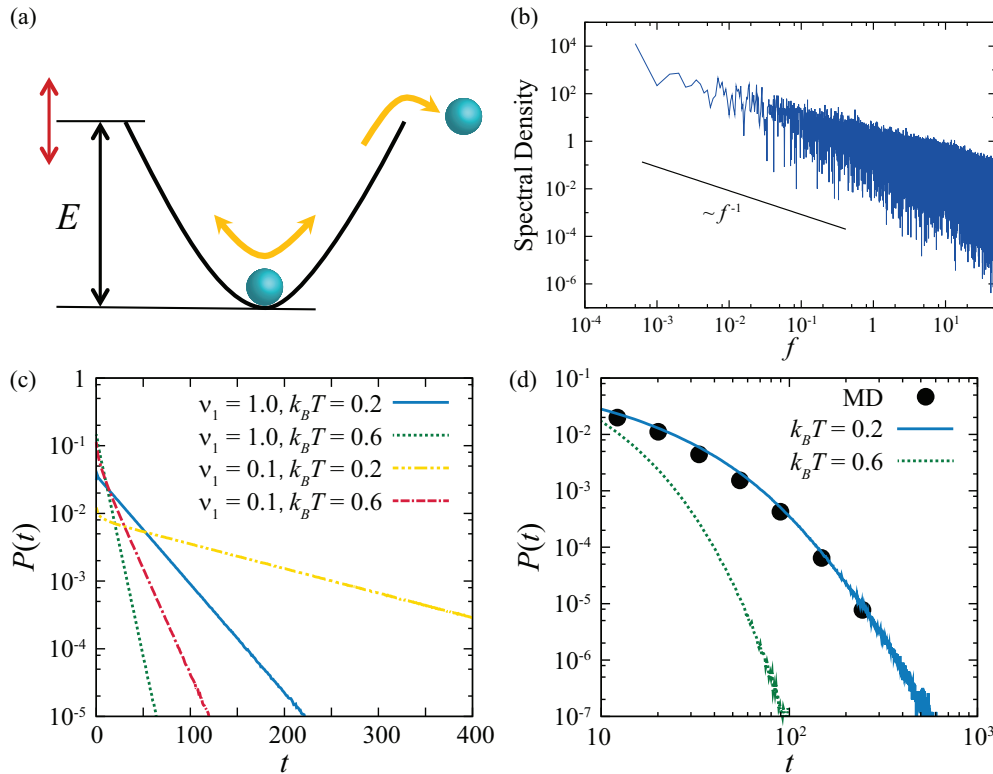


FIG. 6. (Color online) Stochastic model of water permeation. (a) Schematic of the model. A particle (blue circle) is trapped and fluctuates in a potential. The height of potential E fluctuates with $1/f$ noise (red arrow). At a certain moment, the particle escapes from the potential. (b) Power spectra of the $E_N(t)$. Parameter values used in the simulation were $\nu_0 = 50$, $b = 10$, $\alpha = 0.0001$, and $N = 16$. The solid line has slope -1 . (c) PDF of escape times from the fluctuating-threshold potential follows Ornstein-Uhlenbeck noise ($N = 1$) or (d) $1/f$ noise ($N = 16$). The results for Ornstein-Uhlenbeck noise ($N = 1$) and $1/f$ noise ($N = 16$) are shown as single log and log-log plots, respectively. The lines are the results of Langevin simulations. The red circles are the MD simulation results.

the interoccurrence times of the jumping events across the ar/R region. According to an increase of E_0 , PDF changes from nonexponential to exponential distribution (not shown). The nonexponential distribution originated from $1/f$ fluctuations is consistent with that obtained by the MD simulation. Although this model lacks molecular details on water transportation in real AQPs, it avoids unwarranted assumptions about the detailed mechanisms and captures the essential features. This model implies that $1/f$ fluctuations of the potential barrier generate a non-Poisson feature of water transportation within the pore.

IV. CONCLUSION

In summary, we found that amino acids in AQP1 undergo $1/f$ fluctuations by performing MD simulations of membrane-embedded AQP1. Moreover, we found that the interoccurrence times of water molecules crossing the ar/R region in AQP1 follow a nonexponential distribution. To investigate the significance of the $1/f$ fluctuations, we performed restrained

MD simulations of AQP1 and proposed a simple stochastic model of water transportation. The model predicts that water transportation depends on fluctuations of amino acids. These results suggest that $1/f$ fluctuations of amino acids regulate the water transportation in AQPs. Recently, design of using vibrating charge has been proposed for controlling the water transport through CNTs [37,38]. A continuous unidirectional water flow is driven by a vibration charge without osmotic pressure. Our finding would help in designing and developing nanoscale systems for desalination processes.

ACKNOWLEDGMENTS

This work was supported by JSPS KAKENHI (Grant-in-Aid for Challenging Exploratory Research) Grant No. 25630070, Keio University Program for the Advancement of Next Generation Research Projects, and MEXT Grant-in-Aid for the “Program for Leading Graduate Schools.” We thank the RIKEN Integrated Cluster of Clusters (RICC) at RIKEN for the computer resources used for the calculation.

-
- [1] L. S. King, D. Kozono, and P. Agre, *Nat. Rev. Mol. Cell Biol.* **5**, 687 (2004).
- [2] A. Rojek, J. Praetorius, J. Frøkiaer, S. Nielsen, and R. A. Fenton, *Annu. Rev. Physiol.* **70**, 301 (2008).
- [3] C. S. Furman, D. A. Gorelick-Feldman, K. G. V. Davidson, T. Yasumura, J. D. Neely, P. Agre, and J. E. Rash, *Proc. Natl. Acad. Sci. U.S.A.* **100**, 13609 (2003).
- [4] S. Höfing, E. Yamamoto, Y. Hirano, F. Zerbetto, T. Narumi, K. Yasuoka, and M. Yasui, *Biochim. Biophys. Acta* **1818**, 2234 (2012).
- [5] B. L. de Groot and H. Grubmüller, *Curr. Opin. Struct. Biol.* **15**, 176 (2005).
- [6] J. S. Hub and B. L. de Groot, *Proc. Natl. Acad. Sci. U.S.A.* **105**, 1198 (2008).
- [7] M. Yasui, A. Hazama, T.-H. Kwon, S. Nielsen, W. B. Guggino, and P. Agre, *Nature (London)* **402**, 184 (1999).
- [8] B. Wu and E. Beitz, *Cell. Mol. Life Sci.* **64**, 2413 (2007).
- [9] U. K. Eriksson, G. Fischer, R. Friemann, G. Enkavi, E. Tajkhorshid, and R. Neutze, *Science* **340**, 1346 (2013).
- [10] X. Gong, J. Li, H. Lu, R. Wan, J. Li, J. Hu, and H. Fang, *Nat. Nanotechnol.* **2**, 709 (2007).
- [11] B. Corry, *Energy Environ. Sci.* **4**, 751 (2011).
- [12] R. García-Fandiño and M. S. P. Sansom, *Proc. Natl. Acad. Sci. U.S.A.* **109**, 6939 (2012).
- [13] K. Murata, K. Mitsuoka, T. Hirai, T. Walz, P. Agre, J. B. Heymann, A. Engel, and Y. Fujiyoshi, *Nature (London)* **407**, 599 (2000).
- [14] B. L. de Groot and H. Grubmüller, *Science* **294**, 2353 (2001).
- [15] E. Tajkhorshid, P. Nollert, M. Jensen, L. Miercke, J. O’Connell, R. Stroud, and K. Schulten, *Science* **296**, 525 (2002).
- [16] M. Ø. Jensen, E. Tajkhorshid, and K. Schulten, *Biophys. J.* **85**, 2884 (2003).
- [17] B. L. De Groot, T. Frigato, V. Helms, and H. Grubmüller, *J. Mol. Biol.* **333**, 279 (2003).
- [18] F. Zhu, E. Tajkhorshid, and K. Schulten, *Biophys. J.* **86**, 50 (2004).
- [19] A. Berezhkovskii and G. Hummer, *Phys. Rev. Lett.* **89**, 064503 (2002).
- [20] V. J. van Hijkoop, A. J. Dammers, K. Malek, and M.-O. Coppens, *J. Chem. Phys.* **127**, 085101 (2007).
- [21] H. Sui, B. G. Han, J. K. Lee, P. Walian, and B. K. Jap, *Nature (London)* **414**, 872 (2001).
- [22] Y. Hirano, N. Okimoto, I. Kadohira, M. Suematsu, K. Yasuoka, and M. Yasui, *Biophys. J.* **98**, 1512 (2010).
- [23] T. Akimoto, E. Yamamoto, K. Yasuoka, Y. Hirano, and M. Yasui, *Phys. Rev. Lett.* **107**, 178103 (2011).
- [24] E. Yamamoto, T. Akimoto, H. Shimizu, Y. Hirano, M. Yasui, and K. Yasuoka, *J. Phys. Chem. B* **116**, 8989 (2012).
- [25] R. Kagawa, Y. Hirano, M. Taiji, K. Yasuoka, and M. Yasui, *J. Membr. Sci.* **435**, 130 (2013).
- [26] E. Yamamoto, T. Akimoto, Y. Hirano, M. Yasui, and K. Yasuoka, *Phys. Rev. E* **87**, 052715 (2013).
- [27] D. A. Case, T. A. Darden, T. E. Cheatham III, C. L. Simmerling, J. Wang, R. E. Duke, R. Luo, M. Crowley, R. C. Walker, W. Zhang *et al.*, *AMBER 10* (University of California, San Francisco, 2008).
- [28] C.-K. Peng, S. V. Buldyrev, S. Havlin, M. Simons, H. E. Stanley, and A. L. Goldberger, *Phys. Rev. E* **49**, 1685 (1994).
- [29] H. Chen, Y. Wu, and G. A. Voth, *Biophys. J.* **90**, L73 (2006).
- [30] H. Yang, G. Luo, P. Karnchanaphanurach, T. M. Louie, I. Rech, S. Cova, L. Xun, and X. S. Xie, *Science* **302**, 262 (2003).
- [31] W. Min, G. Luo, B. J. Cherayil, S. C. Kou, and X. S. Xie, *Phys. Rev. Lett.* **94**, 198302 (2005).
- [32] W. Li and K. Kaneko, *Europhys. Lett.* **17**, 655 (1992).
- [33] S. M. Bezrukov and M. Winterhalter, *Phys. Rev. Lett.* **85**, 202 (2000).
- [34] Z. Siwy and A. Fuliński, *Phys. Rev. Lett.* **89**, 158101 (2002).
- [35] C. Tasserit, A. Koutsoubas, D. Lairez, G. Zalczer, and M.-C. Clochard, *Phys. Rev. Lett.* **105**, 260602 (2010).
- [36] I. Goychuk, *Phys. Rev. E* **80**, 046125 (2009).
- [37] H. Lu, X. Nie, F. Wu, X. Zhou, J. Kou, Y. Xu, and Y. Liu, *J. Chem. Phys.* **136**, 174511 (2012).
- [38] J. Kou, X. Zhou, H. Lu, Y. Xu, F. Wu, and J. Fan, *Soft Matter* **8**, 12111 (2012).